RESEARCH PAPER

Efficacy and ototoxicity of different cyclodextrins in Niemann–Pick C disease

Cristin D. Davidson[1], Yonatan I. Fishman[1], István Puskás[2], Julianna Szemán[2], Tamás Sohajda[2], Leslie A. McCauliff[3], Jakub Sikora[1,4], Judith Storch[3], Marie T. Vanier[5], Lajos Szente[2], Steven U. Walkley[1] & Kostantin Dobrenis[1]

[1]Dominick P. Purpura Department of Neuroscience, Rose F. Kennedy Center Intellectual and Developmental Disabilities Research Center, Albert Einstein College of Medicine, Bronx, New York 10461
[2]CycloLab Cyclodextrin Research & Development Laboratory Ltd., Budapest H-1097, Hungary
[3]Department of Nutritional Sciences and Rutgers Center for Lipid Research, Rutgers University, New Brunswick, New Jersey 08901
[4]Institute of Inherited Metabolic Disorders, First Faculty of Medicine,Charles University in Prague and General University Hospital in Prague, Prague, Czech Republic
[5]Institut National de la Santé et de la Recherche Médicale,Unit 820; EA4611 Lyon-1 University, Lyon, France

Correspondence

Kostantin Dobrenis, Dominick P. Purpura Department of Neuroscience, Rose F. Kennedy Center Intellectual and Developmental Disabilities Research Center, Albert Einstein College of Medicine, Bronx, NY 10461. Tel: 718-430-2162; Fax: 718-430-8821; E-mail: kostantin.dobrenis@einstein.yu.edu

Abstract

Objective: Niemann–Pick type C (NPC) disease is a fatal, neurodegenerative, lysosomal storage disorder characterized by intracellular accumulation of unesterified cholesterol (UC) and other lipids. While its mechanism of action remains unresolved, administration of 2-hydroxypropyl-β-cyclodextrin (HPβCD) has provided the greatest disease amelioration in animal models but is ototoxic. We evaluated other cyclodextrins (CDs) for treatment outcome and chemical interaction with disease-relevant substrates that could pertain to mechanism. **Methods**: NPC disease mice treated for 2 weeks with nine different CDs were evaluated for UC, and GM2 and GM3 ganglioside accumulation using immunohisto/cytochemical and biochemical assays. Auditory brainstem responses were determined in wild-type mice administered CDs. CD complexation with UC, gangliosides, and other lipids was quantified. **Results**: Four HPβCDs varying in degrees of substitution, including one currently in clinical trial, showed equivalent storage reduction, while other CDs showed significant differences in relative ototoxicity and efficacy, with reductions similar for the brain and liver. Importantly, HPγCD and two sulfobutylether-CDs showed efficacy with reduced ototoxicity. Complexation studies showed: incomplete correlation between CD efficacy and UC solubilization; an inverse correlation for ganglioside complexation; substantial interaction with several relevant lipids; and association between undesirable increases of UC storage in Kupffer cells and UC solubilization. **Interpretation**: CDs other than HPβCD identified here may provide disease amelioration without ototoxicity and merit long-term treatment studies. While direct interactions of CD-UC are thought central to the mechanism of correction, the data show that this does not strictly correlate with complexation ability and suggest interactions with other NPC disease-relevant substrates should be considered.

Introduction

Niemann–Pick type C (NPC) disease is a multiorgan storage disorder characterized by lysosomal accumulation of unesterified cholesterol (UC) and other lipids.

Central nervous system (CNS) neurons widely display polymembranous cytoplasmic storage bodies with intracellular accumulation of GM2 and GM3 gangliosides in addition to UC. Patients exhibit progressive neurological decline. Mutations of the *NPC1* (~ 95% of patients) or

NPC2 gene result in identical disease phenotype.[1] The two encoded proteins, transmembrane NPC1 and soluble luminal NPC2, are thought to interact with UC and/or other lipids in a coordinated fashion to facilitate their egress from late endosomal/lysosomal (LE/LY) compartments.[2]

Therapeutic strategies for NPC disease have included pharmacologic inhibition of substrate accumulation, increasing functionality of defective proteins, and targeting downstream sequelae such as inflammation and oxidative stress.[3] The most efficacious therapy to date has been 2-hydroxypropyl-β-cyclodextrin (HPβCD) which, following even subcutaneous administration to NPC1- or NPC2-deficient mice, delays clinical onset, extends lifespan, and reduces UC and glycolipid accumulation within the CNS and other organs.[4–7]

Several mechanisms by which therapeutic correction is achieved have been proposed,[8,9] but the predominant view is that cyclodextrins (CDs) directly replace the function of NPC proteins within LE/LY compartments.[10] Supporting this idea, HPβCD treatment is also found efficacious in mice deficient in both NPC proteins, but not in other diseases with functional NPC proteins and secondary lysosomal storage of cholesterol.[4,10] Exactly how CD acts to emulate NPC protein function or otherwise mediate CNS correction remains unclear.

CDs form host–guest complexes with a wide range of compounds and are commonly used as excipients. These enzyme-modified starch derivatives are cyclic oligosaccharides toroid in shape with a hydrophobic inner cavity and hydrophilic exterior. There are three common "parent" types, α, β, and γ, composed of 6, 7, and 8 glucose units with increasing inner cavity diameter, respectively. Chemical derivatization of parent CDs is used to change solubility profiles, complexation properties, biodegradability, and toxicity.[11,12] Nearly, all therapy-related studies on NPC animal models have used HPβCD, a βCD derivatized with hydroxypropyl side groups, yet have paid little attention to how different degrees of substitution (DS), that is, the number of hydroxypropyl groups per CD molecule, might affect efficacy.[6,13] Moreover, the potential efficaciousness of any other CD has been rarely investigated[10,14] and since studies show that HPβCD is ototoxic,[15–17] identification of safer alternate CDs is greatly needed.

We administered nine different CDs to $Npc1^{-/-}$ and wild-type (*Wt*) mice, and evaluated reduction of UC and gangliosides, and ototoxicity apparent through auditory brainstem responses (ABRs). To examine whether therapeutic efficacy related to ability of CD to interact with UC and possibly other accumulating lipids, we conducted parallel complexation assays with the same lots of CDs and UC, GM2 and GM3 gangliosides, and other lipids relevant to NPC disease: glucosylceramide, lactosylceramide, sphingosine, oleic acid, bis(monoacylglycero) phosphate (BMP), and 24(*S*)- and 27-hydroxycholesterols (24(*S*)-HC; 27-HC). This is the first time a direct comparison of in vivo efficacy on disease correction and in vitro solubilization of lipids has been performed for a panel of CDs. Indeed, even just broad comparative complexation studies on many of the CDs and substrates examined here is limited. With the exception of oleic acid, posited to be a substrate of NPC1,[18] all lipids we evaluated are elevated in NPC disease[1,19] and viable candidates for consequential interaction with CD. Sphingosine, glucosyl-, and lactosyl-ceramide are precursors for ganglioside synthesis, and sphingosine accumulation may be an initiating factor in the NPC disease cascade.[20] BMP, enriched in internal LE membranes, can modulate cholesterol homeostasis and sphingolipid metabolism.[21,22] Finally, 24(*S*)- and 27-HC traffic out of and into the brain,[23,24] and influence CNS cholesterol homeostasis,[25] providing a potential means to impact neuronal storage from outside the CNS, in light of limited CNS entry of peripherally administered CD.

As CD could also promote membrane interactions, similar to what is observed for NPC2,[2] and thereby facilitate efflux of lysosomal UC,[26] we also evaluated each CD's ability to elicit membrane–membrane aggregation. We found distinct differences among CDs in both efficacy and ototoxicity, including identification of efficacious CDs with reduced ototoxicity, and evidence of substantial and differential complexation with several substrates that could contribute to the outcome of CD-mediated therapy.

Materials and Methods

Animals and treatments

BALB/cNctr-$Npc1^{m1N}$/J heterozygote mice were bred to generate *Wt* and homozygous affected ($Npc1^{-/-}$) progeny and genotyped.[27] From 7–21 days of age, mice were given subcutaneous injections every other day of 2.87 mmol/kg body weight of CD (from a 0.143 mol/L solution) or water alone (vehicle). This dosage corresponds to 4000 mg/kg for HPβCD (Sigma H107, St. Louis, MO), repeatedly shown to be efficacious.[4,5] Additional cyclodextrins included: three other HPβCD products differing in manufacturer and DS; 2-hydroxypropyl-α-CD (HPαCD); 2-hydroxypropyl-γ-CD (HPγCD); sulfobutylether-β-CD (SBEβCD); sulfobutylether-α-CD (SBEαCD); and sulfobutylether-γ-CD (SBEγCD) (Table 1). At 3 weeks of age, tissues were collected for analyses as described in Data S1.

Wt mice used for ABR recordings were given weekly subcutaneous injections of 5.74 mmol/kg body weight of CD (from a 0.286 mol/L solution) or water alone starting

Table 1. Cyclodextrins used.

Cyclodextrin	Abbreviation	Source (cat#)	Average molecular weight (Da)	Average degree of substitution (DS)
2-Hydroxypropyl-α-CD	HPαCD	Sigma Aldrich (39,0690–0)	1180	3.6
Sulfobutylether-α-CD	SBEαCD	Ligand Pharmaceuticals, Inc.[1] (CD-084-87)	1352	2.4
2-Hydroxypropyl-β-CD (Sigma)	HPβCD	Sigma Aldrich (H107)	1396	4.5
2-Hydroxypropyl-β-CD (Trappsol)	Trappsol	CTD, Inc. (THPB-EC)	1541	7.0
2-Hydroxypropyl-β-CD (Kleptose HP)	Kleptose HP	Roquette (346114)	1522	6.7
2-Hydroxypropyl-β-CD (Kleptose HPB[2])	Kleptose HPB	Roquette (346111)	1387	4.3
Sulfobutylether-β-CD (β Captisol)	SBEβCD	Ligand Pharmaceuticals, Inc.[1] (CY-04A-05006.2F)	2163	6.5
Methyl-β-CD[3]	MβCD	Sigma Aldrich (C4555)	1320	13.2
2-Hydroxypropyl-γ-CD	HPγCD	Sigma Aldrich (H125)	1762	8.0
Sulfobutylether-γ-CD (γCaptisol)	SBEγCD	Ligand Pharmaceuticals, Inc.[1] (P186-188-25)	1961	4.2

[1]Cyclodextrins originally obtained from CyDex Pharmaceuticals, Inc. (now Ligand Pharmaceuticals, Inc.).
[2]Kleptose HPB is also known as VTS-270.
[3]MβCD used only in complexation assays; no in vivo work done due to toxicity.

at 8 weeks of age. All animal procedures were carried out according to guidelines approved by the Albert Einstein College of Medicine Institutional Animal Care and Use Committee.

Tissue staining for ganglioside and unesterified cholesterol

Vibratome sections were stained using immunohistochemistry (IHC) to detect GM2 and GM3 gangliosides, and using fluorescent filipin to detect UC essentially as described[28] (Data S1). Widefield digital images were acquired on an Olympus AX70 microscope equipped with a CCD camera (MagnaFire, Optronics). Confocal images were acquired using a Zeiss 510 Meta DuoV2 laser scanning microscope with a 63 × (NA 1.4) objective.

Scoring changes in neuronal accumulation of unesterified cholesterol and gangliosides

Three observers blinded to genotype and treatment independently scored representative coronal tissue sections of brain stained for UC, GM2, or GM3 ganglioside. Each coded slide was given a rating from 0 to 10 (0 = no accumulation, 10 = highest accumulation) for that substrate. Scoring was performed on the dorsomediolateral neocortex at ~ bregma − 2.00 mm. Each slide contained ≥ 3 coronal sections from one mouse (3–8 mice/treatment/stain, except filipin staining for Trappsol where $n = 2$ mice). Scoring was performed at 200×. Data were statistically analyzed with the multigroup nonparametric Kruskal–Wallis test and if appropriate, followed by Dunn's pairwise comparison post hoc test ($P < 0.05$).

Biochemical analysis of gangliosides by TLC

Total lipids were extracted from cerebral hemispheres in choloroform–methanol–20% water[29], and gangliosides were further separated and quantified as in previous studies.[17] Tissue from at least two animals per treatment was analyzed.

Auditory brainstem responses

ABRs elicited by clicks monaurally presented at seven different sound pressure levels (SPLs) were used as an electrophysiological index of hearing thresholds in Wt mice administered different CDs and were assessed at 8, 12, and ~28 weeks of age.

Substrate solubilization by CDs

Biochemical determinations of substrate complexation by CDs were performed in at least one of three ways for each substrate. The first was a mobility shift technique where the target analyte's migration in a high-performance liquid chromatography (HPLC) chromatogram with increasing amounts of CD was recorded, and the data used to calculate a binding constant.[30] The second method also measured mobility shifts, but using capillary electrophoresis and derived an apparent binding constant based on that described.[31,32] Wherever possible, traditional phase solubility studies were conducted to obtain solubility isotherms and a binding constant essentially as described.[33] The methodology employed for each substrate is indicated in Table 2 and details of the techniques are given in Data S1.

Assay of membrane-membrane interactions by different CDs

Large unilamellar vesicles (LUV) composed of 100 mol % egg phosphatidyl choline (EPC) were mixed with increasing concentrations of each CD, and absorbance at 350 nm (light scattering) was monitored (Versamax microplate reader; Molecular Devices, Sunnyvale, CA) over a 30 min period to assess membrane aggregation.[26]

Results

Two-week administration of different CDs to *Npc1*^{−/−} mice results in varied cholesterol and ganglioside reduction in the brain

At 3 weeks, UC accumulation in the brain of untreated *Npc1*^{−/−} mice (detectable as fluorescent filipin-positive puncta in neurons, predominantly perikaryal) was differentially reduced by the nine CDs tested. HPβCD, HPγCD, and SBEγCD all showed comparable effective reduction of UC storage in the cerebral cortex (Fig. 1), and the four commercial HPβCDs showed indistinguishable results (Fig. S1). SBEβCD was less effective while αCD-treated matched untreated *Npc1*^{−/−} mice (Fig. 1). These observations were validated by blind scoring of stained tissue sections (Fig. 2A) which, versus untreated mice, showed statistically significant differences only for the HPβCDs and γCDs. SBEβCD gave intermediate scores, which were not significantly different from either effective CDs or the ineffective αCDs.

In analogous evaluations of reduction of GM2 and GM3 ganglioside accumulation in cortical neurons, different CDs showed a relative efficacy which resembled, but not exactly matched, that for UC. For GM2 (Figs. 1, 2B), very effective statistically significant reduction was again observed with HPβCD and HPγCD, but SBEγCD was less effective and not statistically different from vehicle. SBEβCD and αCDs were indistinguishable from vehicle and significantly different from all HPβCD's and HPγCD. The four different brands of HPβCDs tested (Figs S1, 2B) were all effective and not statistically different from one another. The relative effectiveness of CDs to reduce neocortical GM3 (Figs. 1, 2C and S1) essentially paralleled that seen for UC, again including no significant difference between the different HPβCDs.

Quantitative biochemical determinations of ganglioside content in cerebral homogenates (Fig. 3) showed trends that largely agreed with immunohistochemical data. For GM2, again all HPβCD brands and HPγCD produced values close to that in *Wt* mice, while αCD values were not lower than untreated *Npc1*^{−/−} mice. SBEγCD also showed effectiveness but more so by thin layer chromatography (TLC) measures than by immunostaining and similarly, SBEβCD showed levels by TLC midway between *Wt* and untreated *Npc1*^{−/−} while immunostaining scoring was close to untreated mice. For GM3, TLC data paralleled immunostaining patterns: all HPβCDs and γCDs showed highly effective reduction; SBEβCD exhibited intermediate reduction; and αCDs were indistinguishable from untreated mice.

Table 2. Binding constants (M^{-1}) for CD interaction with Niemann-Pick type C disease related compounds: unesterified cholesterol, brain-relevant oxysterols, glucosylceramide, lactosylceramide, BMP, sphingosine, and oleic acid.

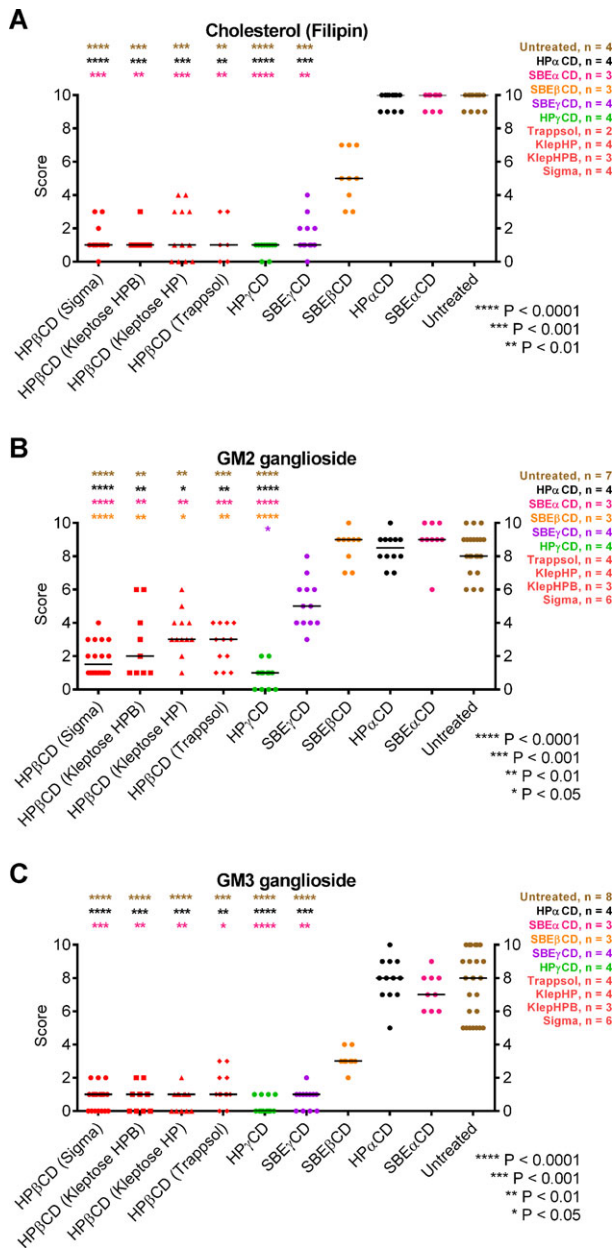| Cyclodextrin	UC	GM2 ganglioside	GM3 ganglioside	24(*S*)-HC	27-HC	Gluc-cer	Lac-cer	BMP	Sphingosine	Oleic Acid
MβCD	7800 ± 110	2410 ± 250	1650 ± 170	400 ± 41	980 ± 18	85	[1]	33	70	1520 ± 25
HPβCD (Sigma)	4072 ± 22	[1]	[1]	117 ± 22	480 ± 14	[1]	[1]	18	3	215 ± 11
Trappsol	3250 ± 80	ND	ND	110 ± 20	455 ± 11	[1]	ND	13	3	220 ± 21
Kleptose HPB	4400 ± 66	[1]	[1]	98 ± 36	462 ± 8	[1]	ND	15	5	245 ± 18
Kleptose HP	3050 ± 52	ND	ND	ND	ND	ND	ND	ND	ND	ND
HPγCD	31 ± 12	[1]	[1]	13	101 ± 3	5	[1]	7	5	22 ± 8
SBEγCD	25 ± 8	[1]; 14 ± 2	26 ± 3	25 ± 8	24	[1]	ND	5	14	13 ± 3
SBEβCD	770 ± 29	10 ± 2; 45 ± 6	61 ± 9	70 ± 29	128 ± 11	5	[1]	3	18	62 ± 7
HPαCD	105 ± 10	60 ± 18; 52 ± 8	36 ± 4	14 ± 3	11	10	[1]	8	8	44 ± 11
SBEαCD	80 ± 13	75 ± 13; 84 ± 9	110 ± 17	7	9	5	ND	6	11	36 ± 9
Method used [2]	1	3	3	1	1	2	2	2	2	1

Values reported are average ± SD.
UC, Unesterified cholesterol; Gluc-cer, glucosylceramide; Lac-cer, lactosylceramide; BMP, Bis (monoacyl-glycero) phosphate; ND, Not done.
[1]Below limit of detection.
[2]Methods used for determination were: (1) solubility isotherm; (2) migration shift by high performance liquid chromatography; and (3) migration shift by capillary electrophoresis.
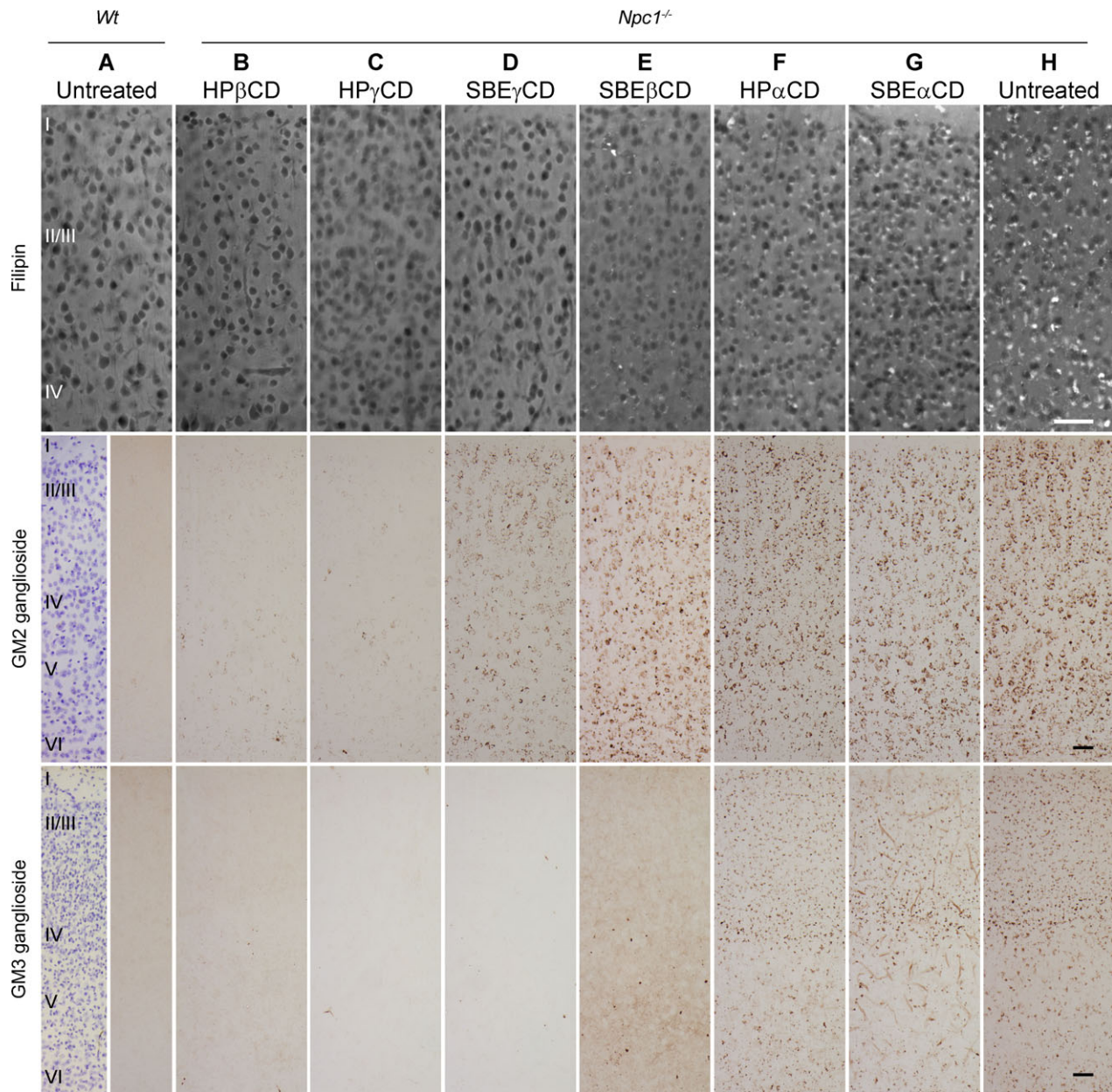
Figure 1. UC, and GM2 and GM3 ganglioside accumulation in the brain cells of 3-week-old mice treated with different CDs. Top row: Sample fluorescence photomicrographs of dorsal neocortex from untreated *Wt* mouse (A), and CD-treated (B–G) and untreated (H) $Npc1^{-/-}$ mice, stained with filipin to detect UC. Virtually, all neurons in untreated $Npc1^{-/-}$ mice show positive cytoplasmic staining of UC (white spots) (H), whereas those in *Wt* mice are negative (A). Note that HPβCD (Sigma) (B), HPγCD (C), and SBEγCD (D) all show highly effective reduction in UC storage, while some UC remains with SBEβCD treatment (E). HPαCD (F) and SBEαCD (G) show UC storage grossly equivalent to untreated mice (H). Middle row: Sample brightfield photomicrographs of dorsal neocortex stained by immunoperoxidase to detect GM2 ganglioside. Dark brown puncta of GM2 immunoreactivity are evident throughout dorsal neocortical neurons in untreated $Npc1^{-/-}$ (H) in contrast to *Wt* (A) mice. The most effective reduction of GM2 in $Npc1^{-/-}$ mice is seen with HPβCD (B) and HPγCD (C). Noticeably more remaining GM2 is evident in $Npc1^{-/-}$ mouse treated with SBEγCD (D), and substantially more with SBEβCD and αCD treatments (E–G) which appear equivalent to untreated $Npc1^{-/-}$ mouse. Bottom row: Sample bright-field photomicrographs of immunoperoxidase stained dorsal neocortex to detect GM3. Dark brown puncta of GM3 immunoreactivity are evident in neurons of untreated $Npc1^{-/-}$ mouse (H), though less abundant than GM2, and absent in *Wt* mouse cortex (A). The relative efficacy of different CDs to reduce GM3 ganglioside parallels UC reduction: HPβCD (B), HPγCD (C), and SBEγCD (D) are nearly indistinguishable from *Wt* (A); SBEβCD (E) shows an intermediate impact; and αCDs (F–G) show no appreciable reduction. *Wt* panels for GM2 and GM3 staining are split: Nissl counterstain in left half reveals cortical layers, marked by roman numerals. Scale bars = 50 μm.

Figure 2. Results of scoring of neuronal UC and ganglioside accumulation in stained samples of dorsomediolateral neocortex from 3-week-old CD-treated *Npc1$^{-/-}$* mice. Tissue sections were scored blind by three independent observers on a scale of 0–10 (10 = greatest accumulation, 0 = no accumulation for that stain). Each point represents one observer's score of sections from one mouse, and horizontal lines show mean value. All stains were found to have evidence of significant differences between conditions (nonparametric ANOVA, $P < 0.0001$). Color-coded asterisks at top of each graph indicate level of significance found in post hoc pairwise statistical comparisons. (A) UC results based on filipin staining. All HPβCDs as well as HPγCD and SBEγCD treatment groups were significantly different from both vehicle and αCDs, and not significantly different ($P \geq 0.05$) from one another. (Note that filipin data for Trappsol treatment was limited to two biological replicates.) SBEβCD produced a range of intermediate values that yielded no significant difference from any group, while αCDs showed no difference from vehicle. (B) GM2 ganglioside scores from immunohistochemical staining. Note that HPβCDs (Sigma, Kleptose HP, Kleptose HPB, and Trappsol) and HPγCD were significantly different from vehicle and αCDs, and these effective CDs showed no difference between them. SBEγCD produced intermediate scores and was not significantly different from any group with the exception of HPγCD. SBEβCD scores were similar to vehicle and statistically different from all HPβCDs and HPγCD. (C) GM3 ganglioside accumulation scores from immunohistochemical staining. The CDs with significantly different results from vehicle were all the HPβCDs, HPγCD, and SBEγCD, with no significant differences among these. SBEβCD produced intermediate values with no significant differences from any groups. Note that GM3 scoring results were remarkably equivalent to UC, with only some differences in confidence (P) level of statistical significance.

HPγCD showed the greatest clearance of hepatocytic UC storage, followed by SBEγCD and then SBEβCD, while αCDs showed no improvement (Fig. 4). However, all CD treatments led to increased UC accumulation in macrophages in *Npc1$^{-/-}$* mice, especially with SBEβCD, secondly HPβCD, and least with the αCDs. CD-injected *Wt* mice also developed striking filipin-positive macrophages with similar relative order of impact seen in *Npc1$^{-/-}$* mice (Fig. 4).

Ototoxic effects of different CDs as measured by ABRs

ABRs were used as an electrophysiological index of hearing thresholds in *Wt* mice. Although vehicle-treated mice had thresholds near 40 dB SPL consistent with normal hearing, mice treated with HPβCD had thresholds ≥100 dB SPL, indicative of extreme hearing loss (Fig. 5A, B). Nearly half the mice treated with HPγCD had a threshold at 88 dB SPL, while all other groups (SBEγCD, SBEβCD, HPαCD) had normal thresholds. Importantly, these trends persisted across the three time points span-

Considering UC and ganglioside data collectively, the overall order of efficacy was: all HPβCDs and HPγCD ≥ SBEγCD > SBEβCD > HPαCD and SBEαCD.

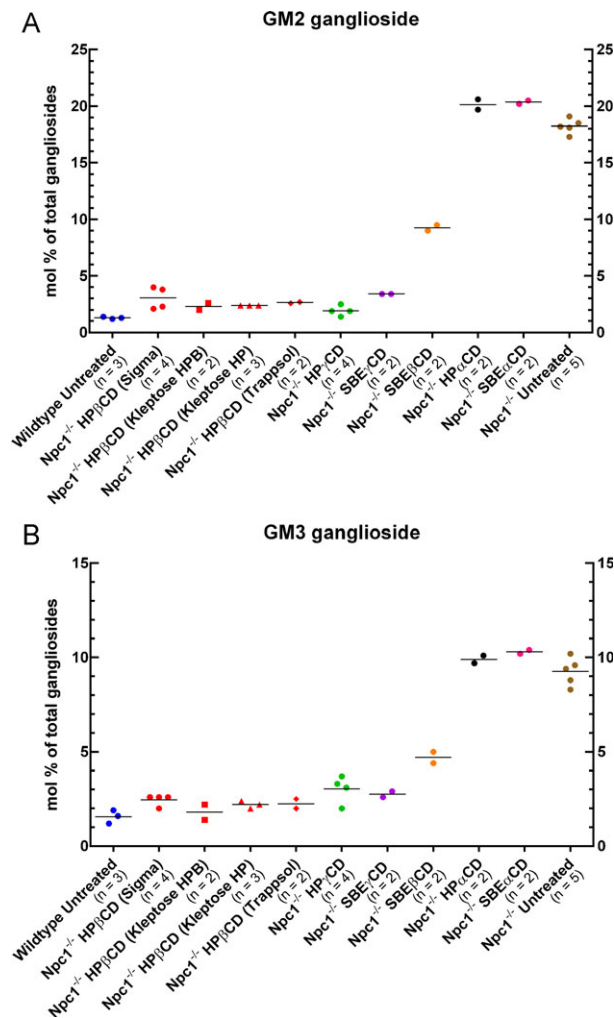## Two-week administration of different CDs results in differential changes in cholesterol accumulation in liver

Filipin staining of liver from untreated *Npc1$^{-/-}$* mice revealed abundant accumulation of UC in hepatocytes and liver macrophages (Kupffer cells). HPβCD and

Figure 3. Biochemical analysis of GM2 and GM3 ganglioside levels in the brain of mice treated with different CDs. Data are expressed as % of total gangliosides after thin layer chromatographic separation of extracts of cerebral homogenates from mice as indicated. While sample size of some groups was insufficient for statistical analysis, individual values are well clustered and confirm reduction of ganglioside levels in *Npc1*$^{-/-}$ mice treated with all the HPβCDs, HPγCD, and SBEγCD to levels approaching that in *Wt* mice. Ganglioside levels in *Npc1*$^{-/-}$ mice treated with SBEβCD showed an intermediate level of reduction, and HPαCD and SBEαCD-treated *Npc1*$^{-/-}$ mice showed no reduction relative to untreated *Npc1*$^{-/-}$ mice. Each pip is a biological replicate and horizontal line shows the mean value.

ning 20 weeks of treatment (Fig. S2). In all cases, mean hearing thresholds were statistically significantly higher for HPβCD-treated mice than for any other group and no significant differences existed between vehicle-treated and SBEγCD, SBEβCD, or HPαCD-treated mice (Fig. 5C). Thresholds for HPγCD-treated mice were intermediate between normal hearing and extreme hearing loss.

## In vitro interaction of NPC-relevant substrates with CDs

To determine whether efficacy of different CDs related to their capacity to interact with relevant substrates, in vitro assays were carried out utilizing the same lots of CDs used in vivo. Methyl-β-CD (MβCD), known for its high cholesterol solubilization, was included as a positive standard. In phase-solubility isotherm studies with UC, MβCD showed the highest binding constant (K; equivalent to equilibrium constant) of 7800 ± 110 M^{-1}, and all HPβCDs were closest to this with Ks between 3050 and 4400 M^{-1}. K$_{SBE\beta CD}$ was notably lower (770 ± 29 M^{-1}), and the γCDs and αCDs about another order of magnitude lower (Table 2). Complexation values (solubilization at a given concentration; Table 3) followed a similar pattern: MβCD > HPβCDs (all with comparable values) >> SBEβCD > SBEγCD > HPγCD and αCDs. Thus, results with the βCDs and αCDs trended toward a positive correlation with degree of UC correction in brain, but γCDs particularly HPγCD, performed better in vivo than the complexation data might predict.

Using the capillary electrophoresis mobility assay, CDs showed either no detectable interaction with ganglioside or Ks $\leq$ 110 M^{-1}, except MβCD with a K $\sim$ 2000 M^{-1}. K values and their relative order in magnitude for different CDs were similar for both gangliosides, with αCDs > βCDs > γCDs given equivalent side groups (Table 2). Furthermore, SBE-CDs had higher Ks than equivalent parent HP-CDs. The data suggested an inverse relationship between K and efficacy in ganglioside reduction, especially for GM2: the most efficacious, HPβCD and HPγCD, showed undetectable interaction; ineffective αCDs had among the highest Ks, and SBEγCD and SBEβCDs were intermediate in both regards. In further support, K values versus biochemical measurements of ganglioside reduction for the CDs, showed a statistically significant correlation and linear relationship (Fig. S3).

Solubility isotherm studies of the oxysterols showed K values about 10-fold lower for 27-HC than UC, and still lower for 24(S)-HC (Table 2). However, the order of relative magnitude for both oxysterols considerably resembled that seen for with UC: MβCD > HPβCDs (all brands similar) > SBEβCD > γCDs $\sim$ αCDs. Complexation values (Table 3) for 24(S)-HC were highest for MβCD, then HPβCD ($\sim$ 0.02 mol/mol), HPγCD and SBE-CDs (0.0007–0.0011 mol/mol), and αCDs (0.0001–0.0003 mol/mol), an order compatible with relative UC reduction in vivo, but differences between the latter two groups in complexation were small compared to UC reduction. Relative CD complexation with 27-HC was quite different, with all HP-CDs showing similar high values. Notably, HPβCD solubilization of 24(S)-HC and 27-HC was equal

C. D. Davidson *et al.*
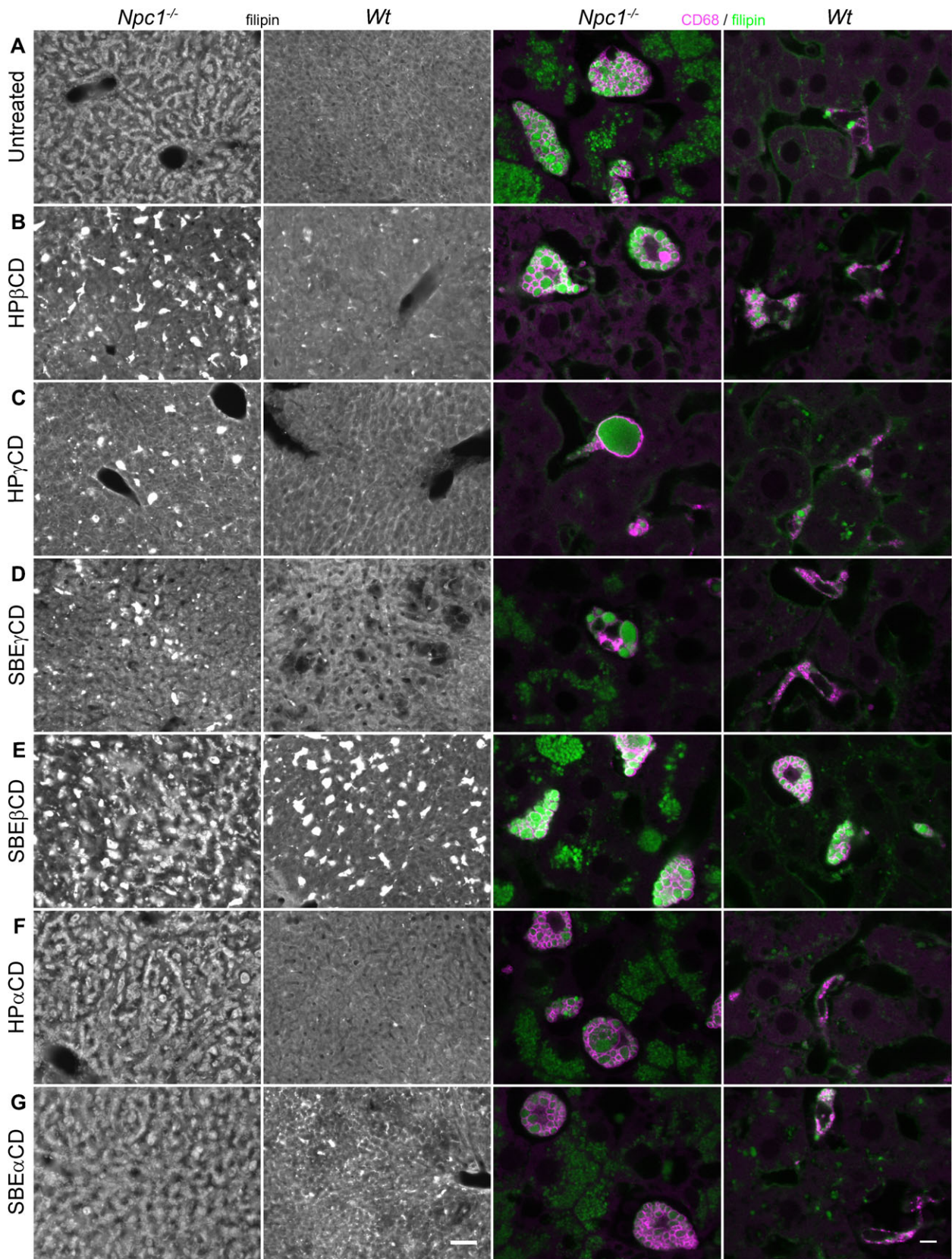
Figure 4. UC accumulation in liver of mice treated with different CDs. First two columns: (A) Filipin labeling of liver from untreated *Npc1*$^{-/-}$ mice revealed widespread accumulation of UC in hepatocytes and Kupffer cells while liver from untreated *Wt* mice exhibited only diffuse filipin labeling. (B–G) *Npc1*$^{-/-}$ mice treated with HPβCD, HPγCD, and SBEγCD showed UC reduction within hepatocytes (B, C, D), while SBEβCD, HPαCD, and SBEαCD treatments showed little to no difference from untreated *Npc1*$^{-/-}$ mice (E, F, G vs. A). Administration of all CDs to *Wt*, as well as disease mice, resulted in elevated UC accumulation in presumptive liver macrophages (Kupffer cells), but hepatocytes remained filipin-negative in *Wt* mice. Note that the accumulation appeared less in *Wt* than in disease mice, but the order of impact by different CDs was similar for the two, for example, in both cases, SBEβCD showed the highest and HPβCD the second highest accumulation in Kupffer cells. Second two columns: Confocal images of liver sections double-labeled with anti-CD68 (magenta), to unambiguously delineate lysosomal membranes of Kupffer cells, and filipin (green). (A) CD68 + Kupffer cells exhibited conspicuous vesicular/vacuolar-like filipin+ labeling in untreated *Npc1*$^{-/-}$ but not *Wt* mice. (B–G) CDs tested in *Npc1*$^{-/-}$ instigated varying degrees of increased UC accumulation in Kupffer cells. *Wt* mice administered different CDs also produced some UC accumulation specifically within Kupffer cells. Scale bars = 50 μm (first two columns), 5 μm (second two columns).
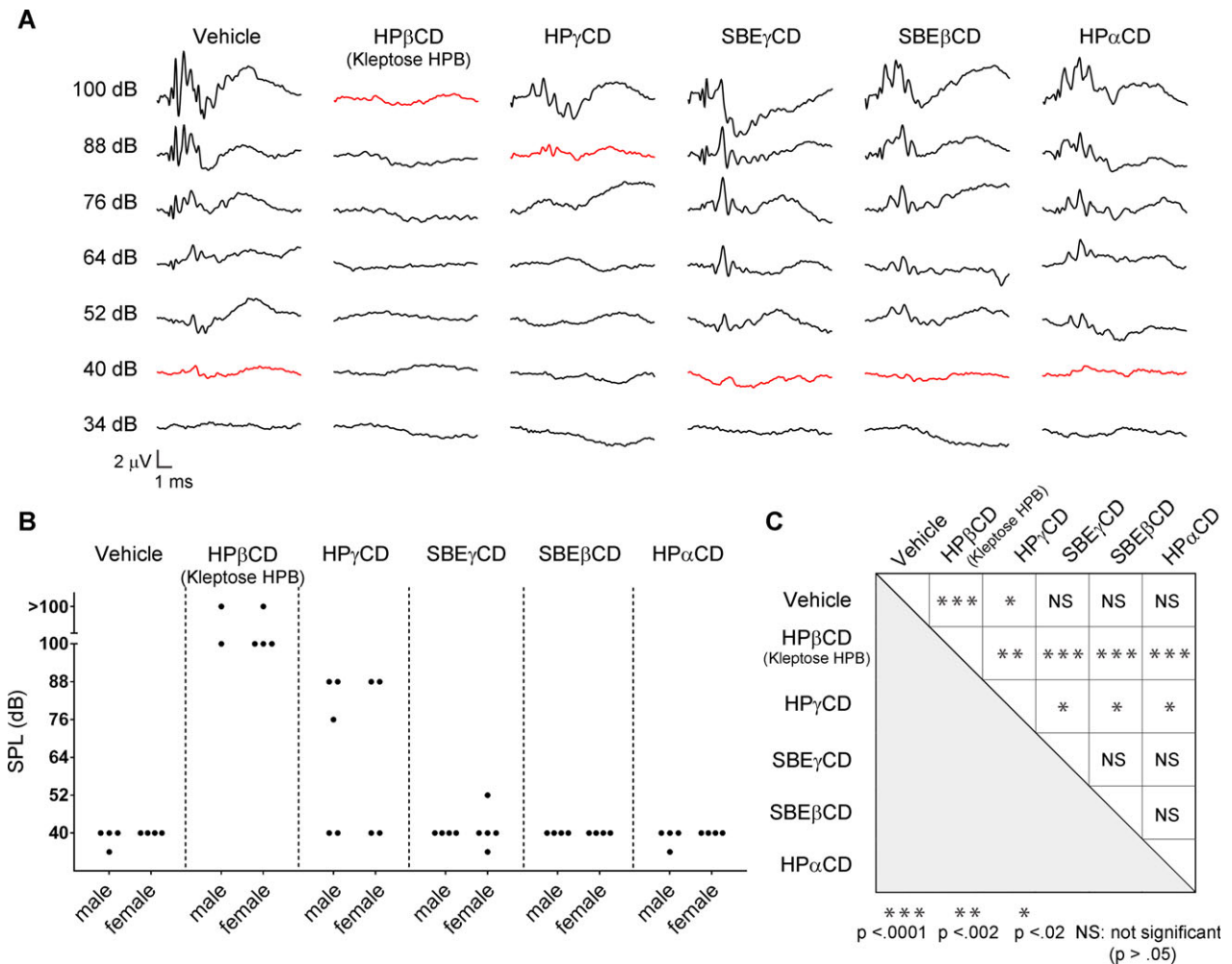
Figure 5. Ototoxicity of different CDs as assessed by auditory brainstem responses (ABR) recordings at 12 weeks of age. (A) Representative ABR recordings from *Wt* mice administered different CDs are depicted. Several stereotypical ABR waveform components are evident, especially at the higher SPLs tested. Differences in waveform morphologies can be attributed to individual differences across mice and to slight variations in the placement of the subcutaneous needle electrodes. Waveforms obtained at threshold are plotted in red. HPβCD and HPγCD traces show pronounced hearing loss while SBEγCD, SBEβCD, and HPαCD traces demonstrate hearing thresholds equivalent to those of vehicle-treated mice (~ 40 dB). (B) Plot of hearing thresholds for individual mice reveals minute variability across mice treated with a particular CD with the exception of HPγCD, in which hearing thresholds were more variable. (C) Two-tailed t-tests comparing mean thresholds for each pair of treatment groups revealed statistically significant differences in threshold only between HPβCD or HPγCD and all other treatment groups.

Table 3. [1]Complexation values of CDs with Niemann-Pick type C disease related compounds: unesterified cholesterol, brain-relevant oxysterols, glucosylceramide, lactosylceramide, BMP, sphingosine, and oleic acid.

Cyclodextrin	UC/CD[2]	UC/CD[3]	24(S)-HC/CD[3]	27-HC/CD[3]	Gluc-cer/CD[3]	Lac-cer/CD[3]	BMP/CD[3]	Sphingosine/CD[4]	Oleic Acid/CD[3]
MβCD	0.2376	ND	0.0852	0.1770	[5]	0.0019	0.0067	1.3222	0.1140
HPβCD (Sigma)	0.0607	0.020	0.0229	0.0402	[5]	[5]	0.0229	0.3263	0.0603
Trappsol	0.0805	0.021, 0.023	0.0190	0.0360	ND	ND	ND	ND	0.0660
Kleptose HPB	0.0610	0.020	0.0177	0.0410	ND	ND	ND	ND	0.0580
Kleptose HP	0.0551	0.024	ND	ND	ND	ND	ND	ND	ND
HPγCD	0.0005	ND	0.0007	0.0621	[5]	[5]	0.0049	0.2059	0.0886
SBEγCD	0.0017	ND	0.0009	0.0004	[5]	ND	[5]	0.3929	0.0167
SBEβCD	0.0058	ND	0.0011	0.0063	[5]	[5]	[5]	1.5889	0.0123
HPαCD	0.0004	ND	0.0003	0.0352	[5]	[5]	0.0104	ND	0.0384
SBEαCD	0.0002	ND	0.0001	0.0031	ND	ND	ND	0.2709	0.0260

UC, unesterified cholesterol; Gluc-cer, glucosylceramide; Lac-cer, lactosylceramide; BMP, Bis (monoacyl-glycero) phosphate; ND, Not done.
[1]Values reported are expressed as mol/mol and were determined from phase solubility isotherms.
[2]Measurements taken with 250 mg CD/mL H_2O.
[3]Measurements taken with 50 mg CD/mL H_2O.
[4]Measurements taken with 10 mg CD/mL H_2O.
[5]Below limit of detection.

to and double that of UC, respectively (compare data columns 2–4, Table 3).

Evidence of stable interaction of the CDs used in vivo with the glycolipids, glucosylceramide, or lactosylceramide, was only detectable for glucosylceramide and limited to HPγCD, SBEβCD, and αCDs, which showed low Ks (5–10 M^{-1}) compared to 85 M^{-1} with MβCD in HPLC migration shift assays (Table 2). Sphingosine, showed an unusually high degree of complexation in phase solubility assays (Table 3) with MβCD and SBEβCD (~ 1.6 mol/mol) and ~ 4- to 8-fold less with other CDs. K values from shift assays (Table 2) ranged from 3 to 18 M^{-1}, other than for MβCD (70 M^{-1}). K values for BMP had a similar range, with HPβCDs the highest second to MβCD (Table 2). Phase solubility complexation values for BMP with the HP-CDs were similar to or greater than with MβCD (Table 3). Lastly, complexation of oleic acid was greater than all other substrates (UC, oxysterols, ceramides, BMP) assayed with 50 mg/mL CD, except for 27-HC:MβCD (Table 3). Following MβCD, the highest complexation and Ks (Table 2) were obtained with the HPβCDs and HPγCD. HP-CDs gave higher values than equivalent parent CDs with SBE substitutions.

## Membrane interaction potential varies among CD derivatives

Using assays to quantify aggregation of phosphatidylcholine LUVs,[26] we found MβCD and all HPβCD brands produced the greatest aggregation (Fig. 6), followed by HPγCD ≈ SBEαCD > SBEγCD > HPαCD ≈ SBEβCD. Only MβCD and HPβCDs values were statistically significantly different from control. Thus, the relative degree of

membrane aggregation trended directly with reduction in neuronal UC and ganglioside accumulation obtained for the β- and γ-CDs but not the αCDs.

Discussion

These studies yield several important findings. One, in evaluating the most extensive variety of CDs to date for UC and ganglioside reduction in the brain of $Npc1^{-/-}$ mice, we find HPγCD as well as HPβCD, the primary CD studied for NPC therapy, are most effective. Furthermore, we show for the first time that SBEγCD also provides significant improvement, along with lesser improvements by SBEβCD. Two, we find that HPβCD is one of the most efficacious CDs, with no significant difference among the four commercial HPβCDs, including Kleptose HPB, which supports its continued use in ongoing clinical trials (NCT01747135 and NCT02534844). Three, we further document HPβCD-induced hearing loss[15–17] and now demonstrate that repeated high-dose administration of two efficacious CDs, SBEγCD and SBEβCD, show no significant ototoxicity, raising important clinical implications for the future. Four, in parallel biochemical studies, we do not find a complete and positive correlation between CD effectiveness in apparent solubilization of cholesterol or ganglioside, or in phospholipid membrane interaction, and ability to reduce the accumulating substrates in the brain. These studies on NPC disease, which for the first time carried out side-by-side comparisons of CDs in vitro and in vivo, show efficacy cannot be fully predicted based on stable interaction in the aqueous phase with a single substrate.

Patient enrollment in a Phase 2/3 clinical trial began in September 2015 and continues use of the Kleptose HPB
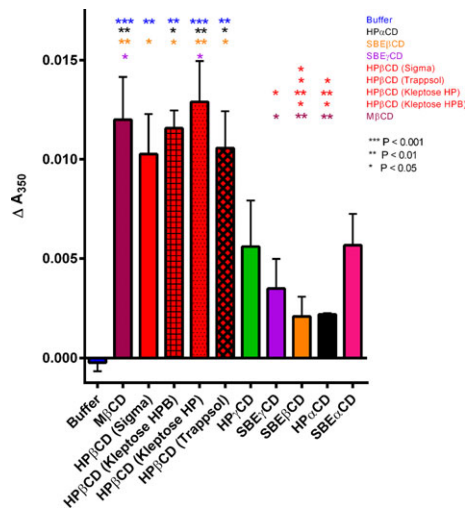
Figure 6. Membrane–membrane interaction of different CDs. Absolute change in absorbance after 30 min incubation period of 100 μmol/L Large unilamellar vesicles (LUVs) with 1 mmol/L CD provides a measure of LUV aggregation (mean ± SE, $N = 3$ experiments). A highly significant statistical difference was found among samples (ANOVA, $P < 0.0001$). Post hoc analysis (Tukey's multiple comparison test) showed that each of the HPβCDs and MβCD were significantly different from control (LUVs with buffer only) ($P < 0.01$; asterisks), and there was no significant difference ($P > 0.05$) among these CDs in pairwise comparisons. While the values for other CDs variably trended above background levels, this aggregation was not found statistically significantly different from control, nor between these other CDs. Similar results were obtained with CDs at 10 μmol/L and 100 μmol/L in three independent experiments (data not shown).

(aka VTS-270) brand of HPβCD, yet there have been few comparative studies on CDs for their efficacy and none for ototoxicity. A recent study found partial rescue of Purkinje cells and modest increase in $Npc1^{-/-}$ mouse survival with HPγCD, but parallel evaluation with HPβCD was lacking.[14] It also found that HPγCD was more effective than HPβCD in correcting molecular and functional abnormalities in induced neural progenitor cells from NPC patients, while we found these CDs indistinguishable in CNS efficacy in mice with treatment beginning at 1 week of age. Whether early intervention could improve long-term outcome remains uncertain and could pose medical complications. The only other comparative report, in this case of 3 CDs, concluded that SBEβCD but not HPαCD matched HPβCD in normalizing cholesterol synthesis in liver and spleen 1 day after subcutaneous injection.[10] While this measure implies correction of UC transport from the lysosome, our direct visualization of UC storage in cells after 2 weeks of treatment clearly showed HPβCD was more effective than SBEβCD in the liver and brain, cautioning that even longer term assessments are desirable given the protracted period of patient

therapy. Beyond these previously considered CDs, we found SBEγCD capable of liver and brain improvements though less efficacious than HPβCD and HPγCD. Thus, HP-substituted CDs had greater impact on storage reduction than did the equivalent SBE-substituted parent rings. We found that the DS for HPβCD (4.5–7.0) made no significant difference in reduction of UC or ganglioside accumulation, in line with reports demonstrating no variance in extending $Npc1^{-/-}$ mouse survival[6] or reducing total cholesterol in $Npc1^{-/-}$ cells.[13]

All β- and γ-CDs produced reduction of UC in hepatocytes, but interestingly led to an increase in vacuolar UC accumulation in Kupffer cells of $Npc1^{-/-}$ mice, as previously observed for HPβCD,[4] and did so in Wt mice as well though to a lesser extent. Thus, given the latter had no deficiency, this suggests that CDs instigated accumulation in the Kupffer cells, not necessarily that a clearance mechanism in principle cannot operate in these cells. This accumulation might result from enhanced sequestration of extracellular CD as a consequence of the enhanced endocytic activity including phagocytosis associated with macrophages. Excessive levels of endocytosed CD in lysosomes, beyond what would typically result in other cell types such as neurons, could then entrap UC and counter its egress from the lysosome in Wt, as well as in $Npc1^{-/-}$ mice where egress is already compromised. This situation may be further aggravated by the fact that macrophages are known to significantly internalize exogenous sources of cholesterol through multiple pathways.[34,35] Alternatively, extracellular precomplexed CD:UC might be accumulated by macrophages, though it has been argued that such complexes are absent from circulation after subcutaneous HPβCD injections.[36] In any case, our findings that HPβCD and SBEβCD showed the largest increase in UC within Kupffer cells and the greatest complexation with UC support the idea that macrophage accumulation of UC is linked to endocytosed CD. Future studies to quantify CD uptake by macrophages and investigate functional consequences would be worthwhile.

Reports of HPβCD-induced ototoxicity with impact on hearing threshold in NPC1 cats and Wt mice[15–17] have been a major concern in moving CD forward as a therapeutic agent. Importantly, we found that HPγCD which was also therapeutically efficacious, showed significantly less ototoxicity than HPβCD in Wt mice, and that the equivalent SBE-substituted βCD and γCD, showed no ototoxicity as assessed by ABR measures. While these findings must be confirmed in $Npc1^{-/-}$ mice, a comparative study on HPβCD-induced toxicity by several criteria on Wt and disease mice, indicated $Npc1^{-/-}$ mice were more resistant, not less, to toxic effects,[37] suggesting these alternate CDs should not produce greater ototoxicity in $Npc1^{-/-}$ mice. It is unclear why HPβCD causes death of

outer hair cells of the cochlea, which underlies the hearing loss,[16] but our observed ototoxicity order of HPβCD > HPγCD > HPαCD matches that reported for hemolysis and toxicity for other cell types.[38–40] In addition, SBEβCD with ~ 7DS, such as we used, showed no hemolysis in contrast to HPβCD at equivalent concentrations.[41] Correlations between hemolytic activity and degree of cholesterol solubilization have been reported (e.g.,[41,42]), but neither our UC:CD complexation data, nor data from any other substrate examined, showed clear predictive power for ototoxicity aside from the observation that HPβCD exhibited both the greatest ototoxicity and UC complexation. Multiple interactions of CD with different hair cell constituents, negative effects at the blood-labyrinth barrier or even disruption of fragile perilymph homeostasis[43] may contribute to toxicity.

Collectively, our therapeutic efficacy and toxicity data suggest that the two effects are to some extent separable and provide a basis for further investigation in *Npc1*$^{-/-}$ mice. Of particular interest is HPγCD which showed equivalent efficacy to HPβCD but reduced ototoxicity and macrophage involvement, and SBEγCD which elicited even fewer side effects but with some reduction in efficacy.

Given the known affinity of βCDs for cholesterol, the therapeutic action of HPβCD has been thought to arise from interaction with UC, be it in extracellular/interstitial fluid, at the plasma membrane or within LE/LYs. Indeed, the findings that both UC solubilization and storage reduction was far higher for the βCDs than the αCDs, and that HPβCD was better than SBEβCD in both regards, support this view. On the other hand, γCDs appeared closer to HPβCD in efficacy but to αCDs in solubilization. Studies pertaining to CNS entry of CDs are inadequate to assert that differential access to neurons could account for these discrepancies and do not suggest γCDs are more effective than αCDs in this regard.[44,45] Relative reduction of UC storage in the brain by different CDs was also very similar to that seen in hepatocytes, further suggesting that blood–brain barrier (BBB) penetrability was not a discriminatory factor. Should the critical mode of CD's action occur within LE/LYs, as many contend,[10,46,47] it could promote UC egress through direct interactions with membranes.[26] This may occur via diffusion of substrate directly from the membrane into the hydrophobic core of CD[48–50] or CD may lower the activation energy for desorption from membrane into aqueous phase[10,51] followed by rapid transfer to an adjacent membrane, that is, movement of accumulated UC from LE/LY multilamellar membranes to the limiting membrane. In fact, we observed a trend for the different β- and γCDs that showed the same order of potency for promoting membrane–membrane interaction (Fig. 6) as observed for reduction of UC storage. Thus, pure aqueous solubiliza-

tion measurements may not be adequately predictive, but the exceedingly low values found for the γCDs, especially HPγCD, calls for consideration of yet other critical mechanisms. Studies directly comparing CDs for UC transfer between adjacent bilayer membranes could be insightful.

It is not clear why GM2 and GM3 accumulate in NPC disease or why HPβCD can counter this. Although speculated,[52] there is no definitive evidence that the NPC proteins directly interact with gangliosides or their metabolic proteins. However, there is evidence of colocalization of gangliosides with UC in LE/LY, particularly striking for GM3, suggesting possible interdependence or association of ganglioside and UC accumulation.[20,53–55] We also found relative reduction of GM2, and even more so of GM3, to parallel efficacy of CDs for UC reduction, further arguing a close link between these compounds. These observations are also compatible with the prevailing view that CD mediates correction from within LE/LYs. Additionally, the CDs showed a significant inverse correlation between their Ks for GM2 or GM3 and their reduction of these gangliosides in brain (Fig. S3), suggesting detrimental effects of CD on ganglioside clearance. In fact, we observed a small increase in % GM2 and GM3 gangliosides in *Npc1*$^{-/-}$ mice treated with αCDs (which showed the highest Ks). It is conceivable that direct interaction with CDs modulated efficiency of ganglioside catabolism.[56] On the other hand, reduction of ganglioside accumulation in LE/LY may arise indirectly. A recent in vitro study showed that elevated membrane cholesterol can inhibit GM2 activator protein function and efficiency of GM2 hydrolysis.[57] Accordingly, CDs more effective at reducing stored UC should also produce greater GM2 reduction, which is what we found.

From the remaining substrates tested, of note were the traditional phase solubility measurements (Table 3) for sphingosine which included values even greater than 1 mol/mol with MβCD and SBEβCD suggesting formation of sphingosine:CD complexes of > 1:1 stoichiometry. The potential therapeutic effects of CD through interaction with sphingosine merit further investigation, as sphingosine is elevated early in NPC disease and has been hypothesized to be an initiating pathogenetic factor for both UC and ganglioside storage.[20]

Of all the substrates evaluated, the relative degree of complexation among CDs with 24(*S*)-HC arguably best approached a correlation with UC storage reduction though this interaction too was imperfect and cannot explain the efficacy findings alone. The range of solubilization values of oxysterols, 0.0001–0.06 mol:mol CD, which resembled and approached levels seen with UC, is worth noting given the levels of HPβCD and the much lower concentration of oxysterols than cholesterol found in the circulation. After a single subcutaneous injection

equal to the one we used, plasma HPβCD peaks at ~ 1.4 or 3.5 mmol/L, depending on mouse age.[7] In *Wt* mice, 24(*S*)-HC and 27-HC are each found at ~ 0.1 μmol/L, respectively, in plasma.[58,59] Thus, the mol oxysterol:mol CD ratio would be 0.00004, well below even the lowest solubilization capacity we measured. Therefore, while BBB penetration of CDs is limited,[17] neuronal accessibility to these oxysterols which purportedly influence cellular cholesterol homeostasis and are the primary sterols that traverse the BBB[23,24] has the potential to be modulated through peripheral interactions with CDs.

In sum, complexation data showed incomplete correlation with efficacy for UC, an inverse correlation for GM2 and GM3, and the closest to a direct correlation for 24(*S*)-HC. Substantial solubilization was also obtained for 27-HC, sphingosine, and oleic acid. Potential influences on efficacy through CD interactions, particularly with sphingosine, gangliosides, and the oxysterols, merit further investigation, particularly in an environment that more closely mimics in vivo conditions. It may well be that the sum of CD interactions with several compounds, in turn altering their availability for endogenous molecular interactions, determines efficacy. Such influences could conceivably account for broader subcellular mechanisms that have been implicated in CD-mediated disease amelioration. These mechanisms include induction of lysosomal exocytosis,[8] TFEB-mediated changes in lysosomal biogenesis,[9] and modulation of the autophagic pathway.[60] Rational development of improved CD-based therapeutics can benefit from understanding the key interactions involved, but our empirical findings already demonstrate that efficacy and toxicity are not wholly inseparable, and viable alternatives to HPβCD are possible. Immediate goals should be long-term efficacy studies of SBE-CDs to fully understand their therapeutic value and validate lack of ototoxicity, with the hope of providing better options for NPC patients and their families.

Author Contribution

CDD, SUW, and KD conceived, designed, and analyzed studies. All authors contributed to design of experiments. TS, LSz, JSz, MTV, YF, IP, JSt, LAM participated in interpretation of the data. CDD and KD wrote the manuscript with contributions from YF, LAM, JS, TS, and LSz, and all authors contributed to editing of the manuscript.

Acknowledgments

Conflict of Interest

SUW is a member of the preclinical SAB for Vtesse, Inc. The other authors have no conflicts.

References

1. Vanier MT. Complex lipid trafficking in Niemann-Pick disease type C. J Inherit Metab Dis 2015;38:187–199.

2. Infante RE, Wang ML, Radhakrishnan A, et al. NPC2 facilitates bidirectional transfer of cholesterol between NPC1 and lipid bilayers, a step in cholesterol egress from lysosomes. Proc Natl Acad Sci USA 2008;105:15287–15292.

3. Rosenbaum AI, Maxfield FR. Niemann-Pick type C disease: molecular mechanisms and potential therapeutic approaches. J Neurochem 2011;116:789–795.

4. Davidson CD, Ali NF, Micsenyi MC, et al. Chronic cyclodextrin treatment of murine Niemann-Pick C disease ameliorates neuronal cholesterol and glycosphingolipid storage and disease progression. PLoS ONE 2009;4:e6951.

5. Liu B, Li H, Repa JJ, et al. Genetic variations and treatments that affect the lifespan of the NPC1 mouse. J Lipid Res 2008;3:663–669.

6. Liu B, Turley SD, Burns DK, et al. Reversal of defective lysosomal transport in NPC disease ameliorates liver dysfunction and neurodegeneration in the npc1-/- mouse. Proc Natl Acad Sci USA 2009;106:2377–2382.

7. Liu B, Ramirez CM, Miller AM, et al. Cyclodextrin overcomes the transport defect in nearly every organ of NPC1 mice leading to excretion of sequestered cholesterol as bile acid. J Lipid Res 2010;51:933–944.

8. Chen FW, Li C, Ioannou YA. Cyclodextrin induces calcium-dependent lysosomal exocytosis. PLoS ONE 2010;5:e15054.

9. Song W, Wang F, Lotfi P, et al. 2-Hydroxypropyl-beta-cyclodextrin promotes transcription factor EB-mediated activation of autophagy: implications for therapy. J Biol Chem 2014;289:10211–10222.

10. Ramirez CM, Liu B, Aqul A, et al. Quantitative role of LAL, NPC2, and NPC1 in lysosomal cholesterol processing defined by genetic and pharmacological manipulations. J Lipid Res 2011;52:688–698.

11. Stella VJ, He Q. Cyclodextrins. Toxicol Pathol 2008;36:30–42.

12. Irie T, Uekama K. Pharmaceutical applications of cyclodextrins. III. Toxicological issues and safety evaluation. J Pharm Sci 1997;86:147–162.

13. Tanaka Y, Yamada Y, Ishitsuka Y, et al. Efficacy of 2-Hydroxypropyl-beta-cyclodextrin in Niemann-Pick disease

type C model mice and its pharmacokinetic analysis in a patient with the disease. Biol Pharm Bull 2015;38:844–851.

14. Soga M, Ishitsuka Y, Hamasaki M, et al. HPGCD outperforms HPBCD as a potential treatment for Niemann-Pick disease type C during disease modeling with iPS cells. Stem Cells 2015;33:1075–1088.

15. Ward S, O'Donnell P, Fernandez S, et al. 2-hydroxypropyl-beta-cyclodextrin raises hearing threshold in normal cats and in cats with Niemann-Pick type C disease. Pediatr Res 2010;68:52–56.

16. Crumling MA, Liu L, Thomas PV, et al. Hearing loss and hair cell death in mice given the cholesterol-chelating agent hydroxypropyl-beta-cyclodextrin. PLoS ONE 2012;7: e53280.

17. Vite CH, Bagel JH, Swain GP, et al. Intracisternal cyclodextrin prevents cerebellar dysfunction and Purkinje cell death in feline Niemann-Pick type C1 disease. Sci Transl Med 2015;7:276ra26.

18. Davies JP, Chen FW, Ioannou YA. Transmembrane molecular pump activity of Niemann-Pick C1 protein. Science 2000;290:2295–2298.

19. Praggastis M, Tortelli B, Zhang J, et al. A murine Niemann-Pick C1 I1061T knock-in model recapitulates the pathological features of the most prevalent human disease allele. J Neurosci 2015;35:8091–8106.

20. Lloyd-Evans E, Morgan AJ, He X, et al. Niemann-Pick disease type C1 is a sphingosine storage disease that causes deregulation of lysosomal calcium. Nat Med 2008;14:1247–1255.

21. Chevallier J, Chamoun Z, Jiang G, et al. Lysobisphosphatidic acid controls endosomal cholesterol levels. J Biol Chem 2008;283:27871–27880.

22. Kolter T, Sandhoff K. Principles of lysosomal membrane digestion: stimulation of sphingolipid degradation by sphingolipid activator proteins and anionic lysosomal lipids. Annu Rev Cell Dev Biol 2005;21:81–103.

23. Heverin M, Meaney S, Lutjohann D, et al. Crossing the barrier: net flux of 27-hydroxycholesterol into the human brain. J Lipid Res 2005;46:1047–1052.

24. Björkhem I, Lutjohann D, Diczfalusy U, et al. Cholesterol homeostasis in human brain: turnover of 24S-hydroxycholesterol and evidence for a cerebral origin of most of this oxysterol in the circulation. J Lipid Res 1998;39:1594–1600.

25. Björkhem I. Crossing the barrier: oxysterols as cholesterol transporters and metabolic modulators in the brain. J Intern Med 2006;260:493–508.

26. McCauliff LA, Xu Z, Storch J. Sterol transfer between cyclodextrin and membranes: similar but not identical mechanism to NPC2-mediated cholesterol transfer. Biochemistry 2011;50:7341–7349.

27. Loftus SK, Morris JA, Carstea ED, et al. Murine model of Niemann-Pick C disease: mutation in a cholesterol homeostasis gene. Science 1997;277:232–235.

28. McGlynn R, Dobrenis K, Walkley SU. Differential subcellular localization of cholesterol, gangliosides, and glycosaminoglycans in murine models of mucopolysaccharide storage disorders. J Comp Neurol 2004;480:415–426.

29. Fujita N, Suzuki K, Vanier MT, et al. Targeted disruption of the mouse sphingolipid activator protein gene: a complex phenotype, including severe leukodystrophy and wide-spread storage of multiple sphingolipids. Hum Mol Genet 1996;5:711–725.

30. Sybilska D, Żukowski J, Bojarski J. Resolution of mephenytoin and some chiral barbiturates into enantiomers by reversed phase high performance liquid chromatography via β-Cyclodextrin inclusion complexes. J Liq Chromatogr 1986;9(2–3):591–606.

31. Wallingford RA, Ewing AG. Capillary electrophoresis.Adv Chromatogr 1989;29:1–76.

32. Rundlett KL, Armstrong DW. Examination of the origin, variation, and proper use of expressions for the estimation of association constants by capillary electrophoresis. J Chromatogr A 1996;721:173–186.

33. Higuchi T, Connors KA. Phase solubility techniques. Pp. 117–212 Advances in analytical chemistry and instrumentation. New York, NY: Wiley Interscience, 1965.

34. Tabas I. Consequences of cellular cholesterol accumulation: basic concepts and physiological implications. J Clin Invest 2002;110:905–911.

35. Wang MD, Kiss RS, Franklin V, et al. Different cellular traffic of LDL-cholesterol and acetylated LDL-cholesterol leads to distinct reverse cholesterol transport pathways. J Lipid Res 2007;48:633–645.

36. Taylor AM, Liu B, Mari Y, et al. Cyclodextrin mediates rapid changes in lipid balance in Npc1-/- mice without carrying cholesterol through the bloodstream. J Lipid Res 2012;53:2331–2342.

37. Tanaka Y, Ishitsuka Y, Yamada Y, et al. Influence of Npc1 genotype on the toxicity of hydroxypropyl-beta-cyclodextrin, a potentially therapeutic agent, in Niemann-Pick Type C disease models. Mol Genet Metab Rep 2014;1:19–30.

38. Leroy-Lechat F, Wouessidjewe D, Andreux JP, et al. Evaluation of the cytotoxicity of cyclodextrins and hydroxypropylated derivatives. Int J Pharm 1994;101 (1–2):97–103.

39. Schonfelder U, Radestock A, Elsner P, et al. Cyclodextrin-induced apoptosis in human keratinocytes is caspase-8 dependent and accompanied by mitochondrial cytochrome c release. Exp Dermatol 2006;15:883–890.

40. Salem LB, Bosquillon C, Dailey LA, et al. Sparing methylation of beta-cyclodextrin mitigates cytotoxicity and permeability induction in respiratory epithelial cell layers in vitro. J. Contr Release 2009;136: 110–116.

41. Rajewski RA, Traiger G, Bresnahan J, et al. Preliminary safety evaluation of parenterally administered sulfoalkyl

ether beta-cyclodextrin derivatives. J Pharm Sci 1995;84:927–932.

42. Kiss T, Fenyvesi F, Bacskay I, et al. Evaluation of the cytotoxicity of beta-cyclodextrin derivatives: evidence for the role of cholesterol extraction. Eur J Pharm Sci 2010;40:376–380.

43. Juhn SK, Hunter BA, Odland RM. Blood-labyrinth barrier and fluid dynamics of the inner ear. Int Tinnitus J 2001;7:78–83.

44. Vecsernyes M, Fenyvesi F, Bacskay I, et al. Cyclodextrins, blood-brain barrier, and treatment of neurological diseases. Arch Med Res 2014;45:711–729.

45. Monnaert V, Tilloy S, Bricout H, et al. Behavior of alpha-, beta-, and gamma-cyclodextrins and their derivatives on an in vitro model of blood-brain barrier. J Pharmacol Exp Ther 2004;310:745–751.

46. Rosenbaum AI, Zhang G, Warren JD, et al. Endocytosis of beta-cyclodextrins is responsible for cholesterol reduction in Niemann-Pick type C mutant cells. Proc Natl Acad Sci USA 2010;107:5477–5482.

47. Abi-Mosleh L, Infante RE, Radhakrishnan A, et al. Cyclodextrin overcomes deficient lysosome-to-endoplasmic reticulum transport of cholesterol in Niemann-Pick type C cells. Proc Natl Acad Sci USA 2009;106:19316–19321.

48. Yancey PG, Rodrigueza WV, Kilsdonk EP, et al. Cellular cholesterol efflux mediated by cyclodextrins. Demonstration Of kinetic pools and mechanism of efflux. J Biol Chem 1996;271:16026–16034.

49. Steck TL, Ye J, Lange Y. Probing red cell membrane cholesterol movement with cyclodextrin. Biophys J 2002;83:2118–2125.

50. Lopez CA, de Vries AH, Marrink SJ. Computational microscopy of cyclodextrin mediated cholesterol extraction from lipid model membranes. Sci Rep 2013;3:2071.

51. Besenicar MP, Bavdek A, Kladnik A, et al. Kinetics of cholesterol extraction from lipid membranes by methyl-beta-cyclodextrin–a surface plasmon resonance approach. Biochim Biophys Acta 2008;1778:175–184.

52. Malathi K, Higaki K, Tinkelenberg AH, et al. Mutagenesis of the putative sterol-sensing domain of yeast Niemann Pick C-related protein reveals a primordial role in subcellular sphingolipid distribution. J Cell Biol 2004;164:547–556.

53. Zervas M, Dobrenis K, Walkley SU. Neurons in Niemann-Pick disease type C accumulate gangliosides as well as unesterified cholesterol and undergo dendritic and axonal alterations. J Neuropathol Exp Neurol 2001;60: 49–64.

54. Gondre-Lewis MC, McGlynn R, Walkley SU. Cholesterol accumulation in NPC1-deficient neurons is ganglioside dependent. Curr Biol 2003;13:1324–1329.

55. Zhou S, Davidson C, McGlynn R, et al. Endosomal/lysosomal processing of gangliosides affects neuronal cholesterol sequestration in Niemann-Pick disease type C. Am J Pathol 2011;179:890–902.

56. Mitsumori R, Kato T, Hatanaka K. g-Cyclodextrin increases hydrolysis of gangliosides by sialidase from *Arthrobacter ureafaciens*: hydrolysis of gangliosides. Int J Carbohydrate Chem 2008;2009:1–4.

57. Anheuser S, Breiden B, Schwarzmann G, et al. Membrane lipids regulate ganglioside GM2 catabolism and GM2 activator protein activity. J Lipid Res 2015;56:1747–1761.

58. Shafaati M, Olin M, Bavner A, et al. Enhanced production of 24S-hydroxycholesterol is not sufficient to drive liver X receptor target genes in vivo. J Intern Med 2011;270:377–387.

59. Karuna R, Holleboom AG, Motazacker MM, et al. Plasma levels of 27-hydroxycholesterol in humans and mice with monogenic disturbances of high density lipoprotein metabolism. Atherosclerosis 2011;214: 448–455.

60. Meske V, Erz J, Priesnitz T, et al. The autophagic defect in Niemann-Pick disease type C neurons differs from somatic cells and reduces neuronal viability. Neurobiol Dis 2014;64:88–97.

Supporting Information

Additional Supporting Information may be found online in the supporting information tab for this article:

Figure S1. UC and GM2 and GM3 ganglioside accumulation in brain cells of 3-week-old mice treated with different commercial preparations of HPβCDs.

Figure S2. Ototoxicity of different CDs as assessed by ABR recordings.

Figure S3. Correlation between reduction of gangliosides in $Npc1^{-/-}$ cerebral cortex and evidence of stable interaction with different CDs.

Data S1. Supplementary Materials and Methods.